Engineering and Technology Journal
Journal homepage: https://etj.uotechnology.edu.iq

Drought in Iraq: remote sensing assessment using LSWI-Index and Landsat imagery

Israa H. Mohammed[a*], **Imzahim A. Alwan**[a], **Abdul Razzak T. Ziboon**[b]

[a] Civil Engineering Dept., University of Technology-Iraq, Alsina'a street, 10066 Baghdad, Iraq.
[b] Construction Engineering and Project Management Department, College of Engineering, Al-Esraa University, Baghdad, Iraq.
*Corresponding author Email: Israa.H.Mohammed@uotechnology.edu.iq

HIGHLIGHTS

- Remote sensing and GIS were used to investigate drought conditions in Iraq from 2000 to 2022.
- The maps were derived using the Land Surface Water Index (LSWI).
- Extreme drought was highest in 2020 and 2021, with 43.9% and 43.3%, respectively.
- Analyzed images show an increasing trend of extreme drought.
- The overall trend of hydrological drought has increased.

ARTICLE INFO

Handling editor: Mahmoud S. Al-Khafaji

Keywords:
GIS
RS
Climate change
Drought
LSWI
Landsat

ABSTRACT

Climate change has significantly increased the risk of drought and natural disasters. Droughts are expected to become more frequent and severe globally, particularly in Iraq, due to decreasing precipitation, rising temperatures, reduced vegetation cover, and water scarcity. The extent and location of drought are primarily influenced by limited precipitation and scarce water resources. In Iraq, drought is a serious and recurring issue exacerbated by the mismanagement of water resources and insufficient precipitation. Drought indicators are utilized to monitor and evaluate drought conditions to address this issue. Drought models typically consider systematic patterns of precipitation shortages, temperature increases, and other factors over decades. This study employs advanced technologies, including remote sensing (RS) and geographic information systems (GIS), to assess drought-affected water surfaces in Iraq from 2000 to 2022 using the Land Surface Water Index (LSWI). The results demonstrate that LSWI effectively identifies hydrological droughts, especially during extreme drought events. Extreme drought conditions were observed in 2020 and 2021, with 43.9% and 43.3% of areas affected, respectively. Severe drought was prevalent in 2000 and 2001, with the highest recorded drought impact being 78.7% and 57.5% of the affected regions, respectively. Additionally, moderate drought conditions were notably high in 2019 and 2003, affecting 9.9% and 9.2% of areas, respectively. The findings of this research can support the development of effective drought alerts using remote sensing. The results confirm the usefulness of LSWI as a rapid and cost-effective index for monitoring changes in land surface water conditions and assessing the impact of drought.

1. Introduction

Iraq is one of the most affected territories worldwide by climate change, along with the dramatic decrease of water inputs in river basins like Tigris and Euphrates [1,2]. Extreme weather events, dust storms, rising mean temperatures, short-term precipitation, and water shortages are featured in Iraq's modern climate conditions [3]. Extreme weather can lead to extreme natural hazards such as heat waves, floods, and droughts. A drought phenomenon is well known as "a long period of lack of precipitations that extended for one session or more, which leads to a decrease in water," precipitation, temperature, water flow, groundwater table, water reservoirs, soil moisture, and snow are examples of drought indices [4]. Depending on the impacts of drought and its characteristics, drought can be classified into different types, such as agricultural drought, hydrological drought, and meteorological drought [5,6]. A prolonged absence of precipitation that is below average is called meteorological drought and can have a significant impact on ecosystems and communities [7]. Water stress that reduces soil moisture and causes crop losses is called agricultural drought. This type of drought severely threatens the security of global food and water supplies and natural ecosystems [8]. A hydrological drought occurs when there is a lack of precipitation, which can cause water shortages and degradation in groundwater, lake, and river water elevation, leading to ecosystem degradation, loss of vegetation cover, and loss of topsoil [9].

The hydrological drought conditions can be monitored and analyzed using different drought indices [10]. These technologies are investigated in various studies. The Land Surface Water Index (LSWI) is one of the hydrological drought

http://doi.org/10.30684/etj.2024.150522.1764
Received 03 June 2024; Received in revised form 20 July 2024; Accepted 23 July 2024; Available online 28 August 2024
2412-0758/University of Technology-Iraq, Baghdad, Iraq
This is an open access article under the CC BY 4.0 license http://creativecommons.org/licenses/by/4.0

indices that utilizes the shortwave infrared (SWIR) and near-infrared (NIR) regions of the electromagnetic spectrum. The LSWI is known to be sensitive to the total amount of water moisture in vegetation and its topsoil, and the water content strongly absorbs light in the SWIR [11]. Two methodological approaches were employed to assess drought conditions using remote sensing techniques and satellite imagery for parameters and conditions like vegetation cover, soil moisture, evaporation, and rainfall [12,13]. In recent years, the benefits of using remote sensing data in observing and monitoring drought conditions have greatly enhanced drought management and decreased its effects [14,15]. Several studies have utilized remote sensing data to identify droughts' duration and location. For example, Chandrasekhar et al. [16] compared the results of the Normalized Difference Vegetation Index (NDVI) and Land Surface Water Index (LSWI). To assess the impact of rainfall, the NDVI for 2002 was missing from the MODIS VI product, so it is not available for analysis, but the MODIS VI data and the SWIR and NIR reflectance values were used to obtain the LSWI for 2005. A strong correlation between NDVI and LSWI is found for most processed data with a delay of two weeks [16]. Xiang et al. [17] have studied agricultural irrigation in China through an integrated approach of statistical, annual mean rainfall, land cover analysis from the satellite MODIS, and the surface reflectance values, This methodology proved promising method in drawing maps of irrigated areas and observing their annual fluctuations. LSWI values for agricultural pixels were compared with the surrounding forest pixels that have the same NDVI. These results explain the effective range of this method in drawing the maps of the irrigated areas and observing their annual changes [17].

Dong et al. [18] introduce a technique that combines NDVI and LSWI to extract information on seasonal variation in wetlands, which is different from the previous methods that do not consider seasonal variation in wetland information. The proposed efficient drought extraction using the NDVI and LSWI approaches will be aided by seasonally independent management of wetland design, monitoring, planning, and ecological management [18]. Khalaf studied the hydrological drought in the Middle Euphrates region of Iraq [19]. This study used the LSWI to analyze drought rates based on crop water content and water at the topsoil. This study used the difference between the NIR and SWIR1 spectral values of Landsat images TM, ETM+, and OLI from 1988, 1993, 2000, 2005, 2010, and 2018. The study results show that the area was affected by severe agricultural and hydrological drought between 1988 and 2018. The drought areas were 17% to 23% of the total area [19, 20]. Because of the lack of long-term hydrological data (e.g., precipitation, streamflow, groundwater levels, water lost through evaporation), it is necessary to find another method to study the long-term hydrological drought. One possible method is using natural resources such as Landsat and satellite images based on hydrological drought indices such as LSWI. State-of-the-art technologies such as remote sensing and geographic information systems (GIS) are used to investigate the effects of drought on the water surface in Iraq by creating comprehensive drought maps at different periods using the LSWI index and Landsat image data for the years (2000-2022).

2. Study area

Iraq Figure 1 is the eastern border of the Arab homeland and is located in southwest Asia. It borders Syria and Jordan to the west, Iran to the east, Turkey to the north, and Saudi Arabia and Kuwait to the south. Iraq lies between the latitudes ($29^{\circ}00'N$ to 37° 15′N) and longitudes ($38^{\circ}45'E$ to $48^{\circ}25'E$) and has a land area of 438,320 km^2 [21].

The climate in Iraq varies significantly due to the country's topography and geographical location. Iraq has both continental and subtropical weather. Most winters are below-freezing, with little to no rainfall. Rainfall occurs from September to May, with the highest precipitation volumes in December and March. Iraq has short periods of spring and fall, followed by a hot and dry summer with temperatures exceeding 50 °C. The area's evaporation rate increases dramatically due to climatic change factors such as high temperatures, low precipitation, and strong winds. The Euphrates and Tigris are rivers that stream through Iraq and extend from northwest to southeast (Figure 1).

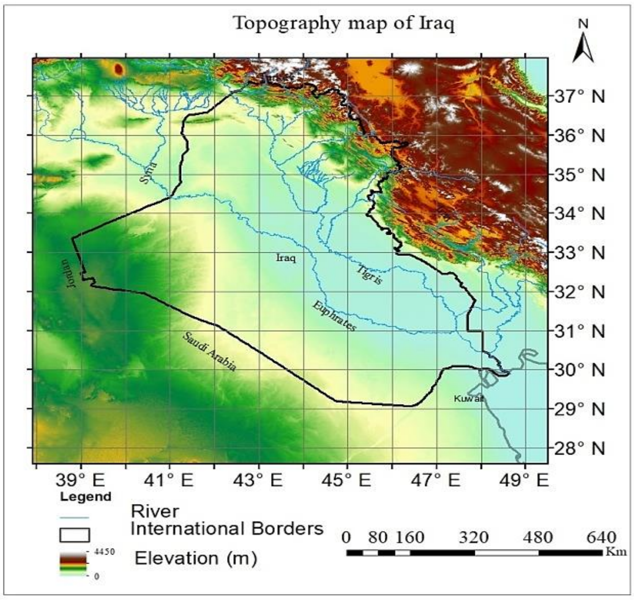

Figure 1: Topographic of Iraq

3. Methodology

The objectives of this study can be achieved with the assessment of drought conditions in spatiotemporal domine for the Iraqi regions for the study time from (2000 to 2022). Two different Landsat sensors with a (30 m) spatial resolution were used to create the remote sensing datasets: the L7 Enhanced Thematic Mapper Plus (ETM+) and the L8 Operational Land Imager (OLI). The Landsat 7 and 8 TM Collection 1 Tier 1 composites were created from orthorectified Tier 1 scenes using the calculated top-of-atmosphere (TOA) reflectance and are thus geometrically and radiometrically matched see Table 1 [22, 23]. The Landsat satellite images for the study region are acquired using Google Earth Engine (GEE), which is also used to apply the LSWI index and to determine the mean of LSWI every year the study was conducted. In this work, a Geographic Information System (GIS) was used to generate maps showing the spatial distribution of LSWI classes. Figure 2 represents the methodology of this research.

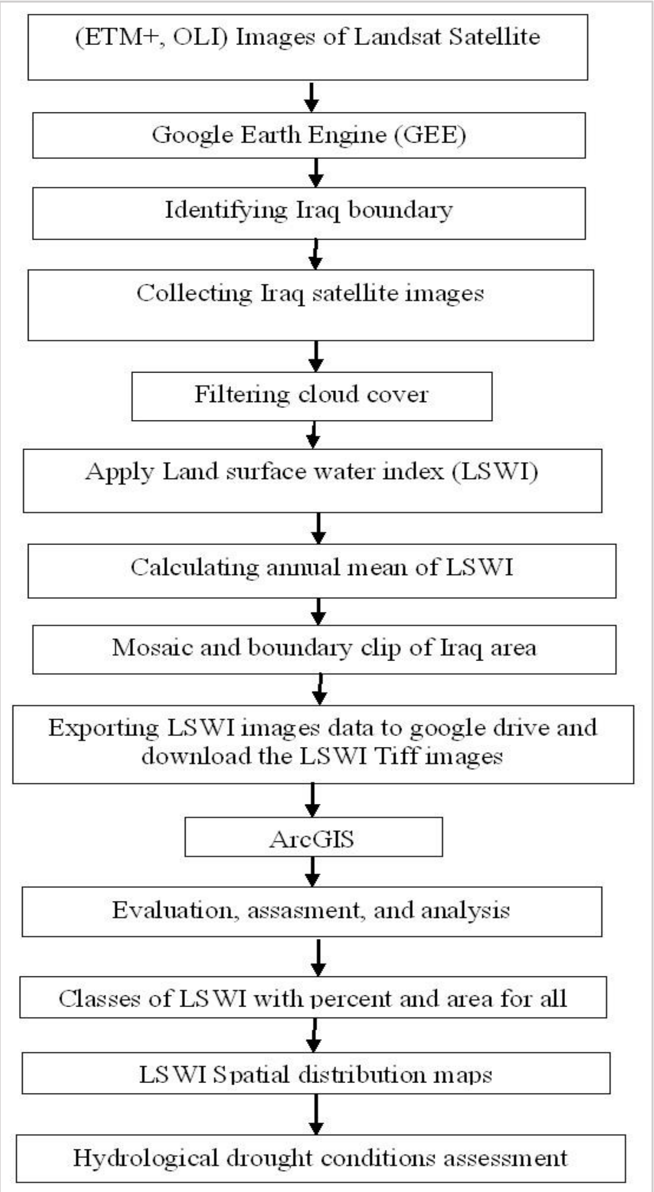

Figure 2: Flowchart of the LSWI calculation

Table 1: Data used and source

No.	The Data used parameter	Source
1	L7 enhanced thematic mapper plus (ETM+)	Google. "Landsat 7 Collection 1 Tier 1 8-Day TOA Reflectance Composite."
2	L8 operational land imager (OLI)	Google. "USGS Landsat 8 Collection 2 Tier 1 TOA Reflectance."

Temperature and precipitation are the main climate factors that directly influence the drought. In this study, 27 meteorological station temperature and precipitation data were used. These stations are distributed all over Iraq. Figure 3 and Table 2 summarize the location and names of the stations.

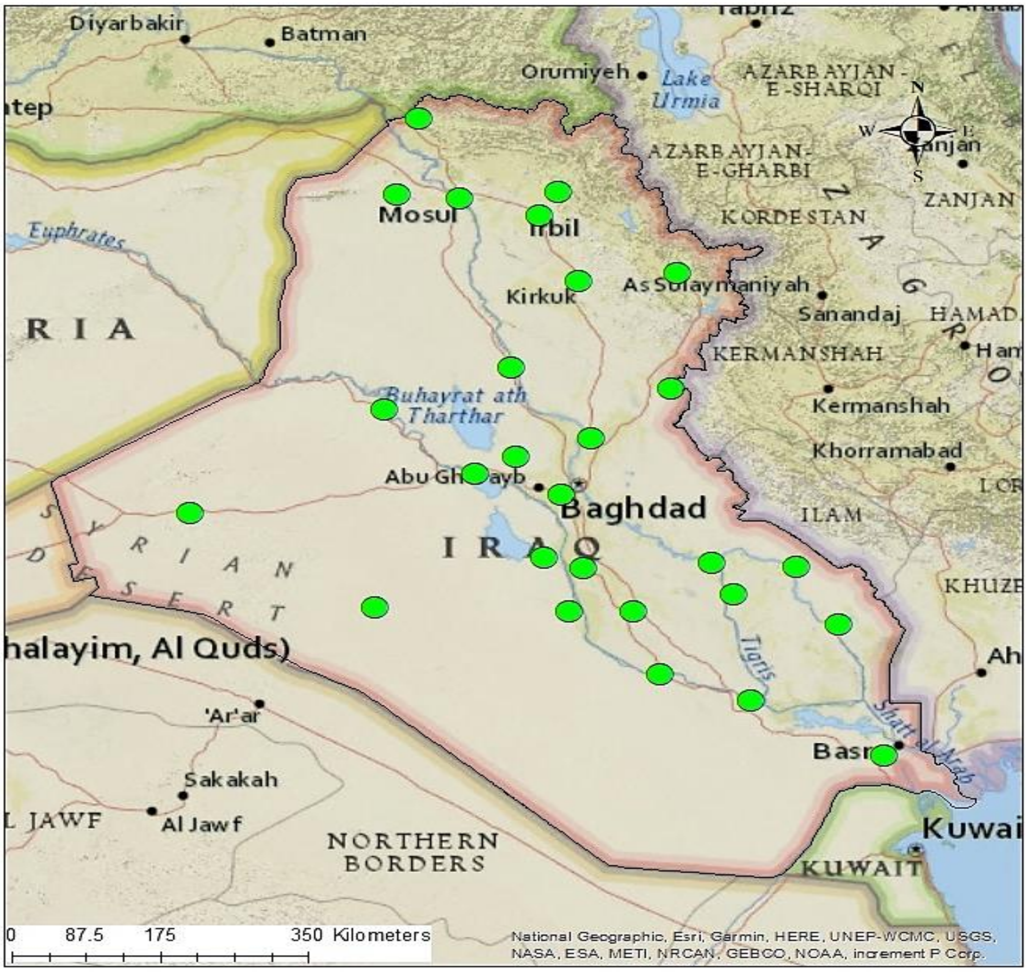

Figure 3: Point location and distribution

Table 2: Points coordinates, availability, and references

Station name	Coordinates		Available	Refe.
	Longitude	Latitude		
Ali-Algharbi	47	32	yes	IMO*
Al-Khalis	45	34	yes	IMO
Amarah	47	32	yes	IMO
Arbil	44	36	yes	IMO
Baghdad	44	33	yes	IMO
Basrah	48	30	yes	IMO
Diwaniya	45	32	yes	IMO
Hadithah	42	34	yes	IMO
Heet	44	34	yes	IMO
Hella	44	32	yes	IMO
Kerbela	44	33	yes	IMO
Khanaqin	45	34	yes	IMO
Kirkuk	44	35	yes	IMO
Kut	46	33	yes	IMO
Kut-Al-Hai	46	32	yes	IMO
Mosul	43	36	yes	IMO
Najaf	44	32	yes	IMO
Nasiriya	46	31	yes	IMO
Nukaib	42	32	yes	IMO
Ramadi	43	33	yes	IMO
Rutbah	40	33	yes	IMO
Salahaddin	44	36	yes	IMO
Semawa	45	31	yes	IMO
Sulaimaniya	45	36	yes	IMO
Tel-Afer	42	36	yes	IMO
Tikrit	44	35	yes	IMO
Zakho	43	37	yes	IMO

* Iraqi meteorological organization and seismology

4. Land surface water index (LSWI)

Land Surface Water Index (LSWI) is an instrument for monitoring drought conditions [24]. In areas with low precipitation, the relationship between LSWI and total precipitation is more significant [25]. The LSWI plays a significant role in monitoring the vegetation cover and soil water content during the different stages of plant growth [26].

LSWI is defined as follows:

$$LSWI = \frac{(NIR-SWIR)}{(NIR+SWIR)} \tag{1}$$

where: NIR is the near-infrared spectral reflectance band for satellite images.

SWIR in Equation 1 is a satellite image's short-wave infrared reflectance band [27, 28]. Combining the two spectral bands (SWIR and NIR) can generate the LSWI index. It is sensitive to the water content in vegetation land cover and the water and moisture in its topsoil. In contrast, the band SWIR is sensitive to the soil moisture and the water content in the vegetation cover. The reflectance of band SWIR is decreased, and the absorption increases with increased water content in the soil and the vegetation's water content, leading to an increase in the LSWI values [29]. There are four classes for the severity of the LSWI index. The first class can be distinguished as the extreme drought, which ranges between ($LSWI \leq -0.1$). The second class is the severe drought, which ranges between ($0 < LSWI \leq -0.1$); the third class is the moderate drought, which varies between ($-0.1 < LSWI \leq 0$); and the fourth class is the no drought and has the range between ($0.1 < LSWI$) [30, 31].

5. Results and discussion

Figure 4 represents the trend and time series of temperature and precipitation for the study period from the year 2000 to the year 2022. The temperature data in the figure represent the mean annual temperatures for 12 months and 27 weather stations distributed all over Iraq, while the precipitation data represent the mean annual precipitation of the 27 weather stations.

There is an increased trend in mean annual temperatures from the year 2000 to the year 2022, with the highest temperature being 24.6 °C in 2010 and the lowest temperature being 22.3 Figure 4a. As for precipitation, the trend is a decline in annual precipitation values throughout Iraq, which means a lack and scarcity of water and a decline in water bodies.

The precipitation and temperature data are noisy and need to be smoothed to study the waves in the data. The average mean smooth method is used to smooth the precipitation and temperature data from Figure 4 (a and b). Figure 4c illustrates a negative relationship between temperature and precipitation. A drought assessment was carried out in the study area using the Land Surface Water Index (LSWI). LSWI results were calculated for each year of the study period (2000–2022). The analysis of the results of LSWI shows that the study area suffered from extreme drought in years (2020 and 2021), While severe drought dominated in years (2000 and 2001). The results also showed moderate drought prevailed over the years (2019 and 2003). Table 3 shows the maximum, mean, and minimum LSWI values for every conducted year from (2000-2022) in the study area.

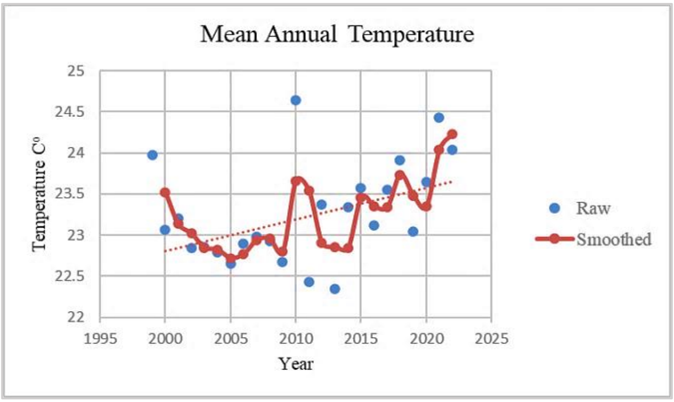

(a)

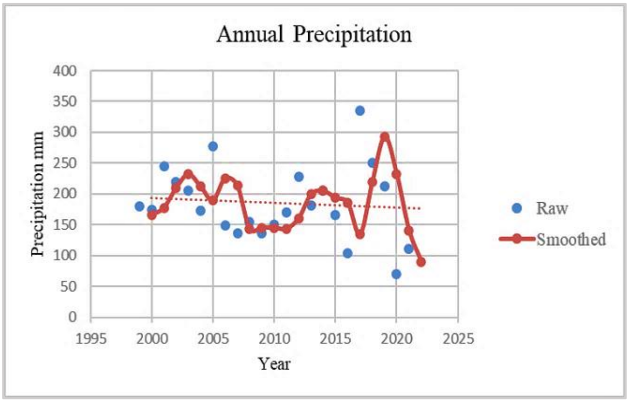

(b)

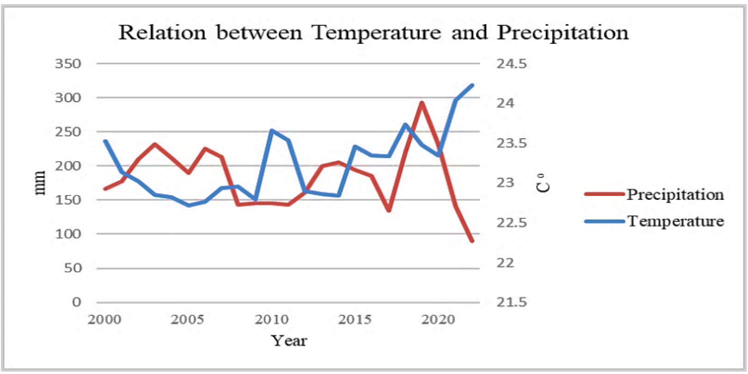

(c)

Figure 4: The trend and time series of (a) Temperature, (b) Precipitation, (c) relation between Temperature and Precipitation

Table 3: Max., Mean, Min, and Standard deviation STD of LSWI values for every year the study was conducted

Year	Max	Mean	Min	STD	Year	Max	Mean	Min	STD
2000	0.75	-0.07	-0.65	0.00746361	2012	0.63	-0.07	-0.37	0.005324
2001	0.78	-0.06	-0.71	0.006474913	2013	0.65	-0.06	-0.28	0.006321
2002	0.81	-0.06	-0.62	0.004329325	2014	0.72	-0.06	-0.24	0.004213
2003	0.87	-0.06	-24	0.007645743	2015	0.62	-0.07	-0.37	0.000546
2004	0.74	-0.06	-0.42	0.002654936	2016	0.67	-0.06	-0.38	0.007395
2005	0.99	-0.06	-0.3	0.00185038	2017	0.64	-0.07	-0.34	0.004792
2006	0.76	-0.06	-0.39	0.001021203	2018	0.76	-0.06	-0.34	0.009964
2007	0.72	-0.06	-0.5	0.005559327	2019	0.67	-0.04	-0.36	0.00512
2008	0.72	-0.07	-0.39	0.001516566	2020	0.7	-0.06	-0.39	0.007757
2009	0.65	-0.07	-0.43	0.00130339	2021	0.72	-0.06	-0.38	0.008785
2010	0.62	-0.07	-0.28	0.002584411	2022	0.59	-0.07	-0.32	0.008564
2011	0.85	-0.07	-0.33	0.006108345					

Based on the LSWI results, the results for the area were divided into four classes: extreme, severe, moderate, and no drought. The percentage and area of each class were calculated and shown in Table 4.

Table 4: The percent and area of the LSWI classes

year	Class 1 Extreme Drought		Class 2 Severe Drought		Class 3 Moderate Drought		Class 4 No Drought	
	Area (Km^2)	*Area (%)*	*Area (Km^2)*	*Area (%)*	*Area (Km^2)*	*Area (%)*	*Area (Km^2)*	*Area (%)*
2000	52721.57	12.0	345033.6	78.7	27779.98	6.3	12778.86	2.9
2001	134005.3	30.6	251979.8	57.5	32494.98	7.4	19833.97	4.5
2002	155101.2	35.4	239452.4	54.6	28347.83	6.5	15412.63	3.5
2003	129892.4	29.6	241807.8	55.2	40246.54	9.2	26367.23	6.0
2004	141734.3	32.3	243748.9	55.6	30319.26	6.9	22511.55	5.1
2005	154003.2	35.1	237983.4	54.3	27270.36	6.2	19056.95	4.3
2006	145297.5	33.1	234112	53.4	35709.22	8.1	23195.28	5.3
2007	150273.8	34.3	234356.4	53.5	32480.63	7.4	21203.11	4.8
2008	151542.1	34.6	242924.4	55.4	30007.81	6.8	13839.68	3.2
2009	154685.1	35.3	246260.4	56.2	23530.73	5.4	13837.73	3.1
2010	170619.4	38.9	233055.9	53.2	21509.02	4.9	13129.65	3.0
2011	163351.3	37.3	235452.3	53.7	24682.59	5.6	14827.9	3.4
2012	163532.2	37.3	234016.2	53.4	25823.36	5.9	14942.26	3.4
2013	152844	34.9	238006.3	54.3	28953.62	6.6	18510.05	4.2
2014	140799.6	32.1	246059.9	56.1	32825.57	7.5	18628.91	4.3
2015	158147.9	36.1	237063.2	54.1	29278.1	6.7	13824.78	3.2
2016	156334	35.7	231970.9	52.9	33134.19	7.6	16874.93	3.8
2017	157595.7	35.9	234843.9	53.6	28144.43	6.4	17729.93	4.0
2018	149077.3	34.0	246642.9	56.3	28520.24	6.5	14073.52	3.2
2019	116964.7	26.7	250617.9	57.2	43477.84	9.9	27253.56	6.2
2020	192440.1	43.9	184748.9	42.1	35844.47	8.2	25280.62	5.8
2021	189839.9	43.3	189208.1	43.2	37071.27	8.5	22194.67	5.1
2022	148876.9	33.9	242902.4	55.4	30620.57	6.9	18691.85	3.6

Table 4 shows that the unaffected area increased from 12,778.86 km² (2.6% of Iraq's total area) in 2000 to 18,691.85 km² (3.6% of Iraq's total area) in 2022, reflecting a net increase of 5,913 km² (1% of Iraq's total area). The maximum unaffected area was recorded in 2019, with 27,253.56 km². The area classified as moderate drought increased from 27,779.98 km² (6.3% of Iraq's total area) to 30,620.57 km² (6.9% of Iraq's total area), representing a gain of 0.6% of Iraq's total area. The maximum extent of moderate drought occurred in 2019, affecting 9.9% of Iraq's total area. The maximum area of severe drought was recorded in the first year of the study, 2000, with 345,033.6 km², representing 78.7% of Iraq's total area. This category experienced the most significant reduction, decreasing to 242,902.4 km² in 2022, a decrease of 23.3% of Iraq's total area. The extreme drought area was initially 52,721.57 km² (12% of Iraq's total area) and expanded to 148,876.9 km² by 2022, representing 33.9% of Iraq's total area, an increase of 21.9%.

Overall, the drought years (2020 and 2021) had the highest percentage of areas affected by extreme drought (43.9 and 43.3%, respectively), while the drought years (2000 and 2001) had the highest percentage of areas affected by severe drought (78.7 and 57.5%, respectively). The highest percentage of regions suffering from moderate drought was in the drought years (2019 and 2003) with 9.9 and 9.2%, respectively. Figure 5 shows the time series for each class, and we can observe an increasing trend in the area of extreme, moderate, and no drought, while in severe drought, there is a decline in the area of drought in favor of extreme drought. The spatial distribution maps of the classes of LSWI for Landsat images are illustrated in Figure 5.

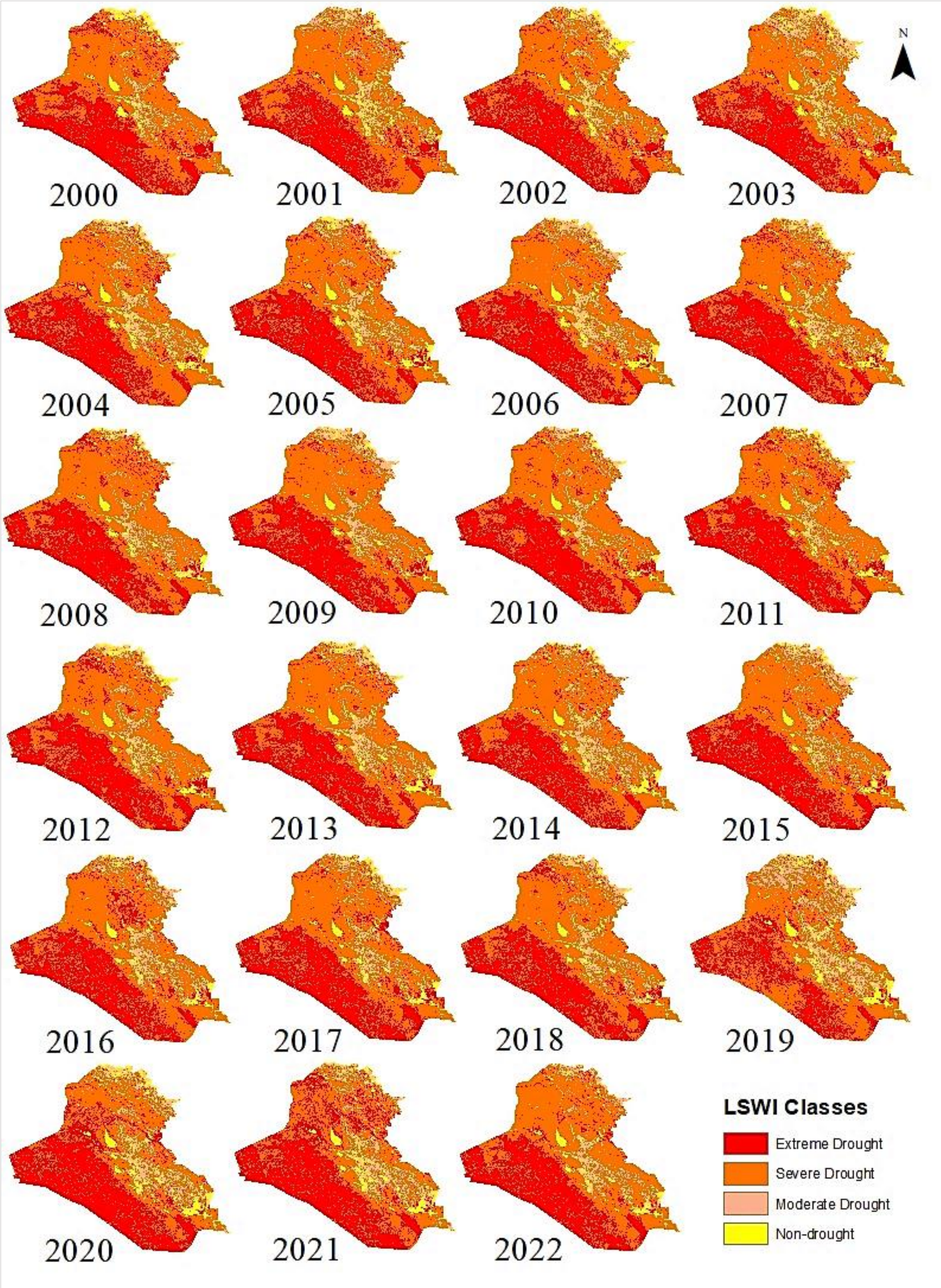

Figure 5: The spatial distribution of LSWI classes

According to Figure 5, the northern part of Iraq is the least affected by the drought, as this region receives the highest volume of rainfall, especially from September to May, with the most significant volume of precipitation between December and March. The river's proximity also helps mitigate the effects of drought in the central areas of Iraq. The western regions of Iraq have deficient precipitation compared to other parts. The lack of water sources such as rivers and lakes and the lack of vegetation are among the most essential reasons for extreme drought in this part. Over the years, these reasons have led to the inability of the population to live in this area, which results in social and economic losses that were not benefiting from this part in agricultural and industrial fields, which are more than a third of the area of Iraq. It is also one of the most important reasons for the difficulty of security control over this part.

Figure 6 illustrates the time series of the LSWI for each class, presented in square kilometers (km²) and percentages. Specifically, Figure 6a depicts the extreme drought area in km², while Figure 6b shows the extreme drought area as a percentage. Figure 6c represents the severe drought area in km², and Figure 6d presents it as a percentage. Similarly, Figure 6e illustrates the moderate drought area in km², with Figure 6f showing it as a percentage. Finally, Figure 6g represents the non-drought area in km², and Figure 6h shows the non-drought area as a percentage.

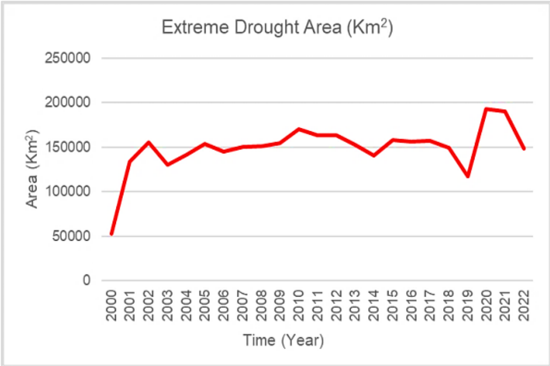

(a)

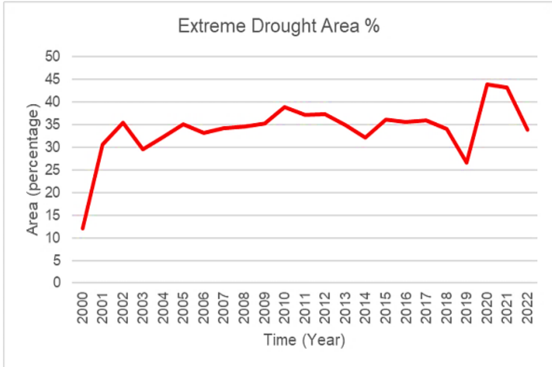

(b)

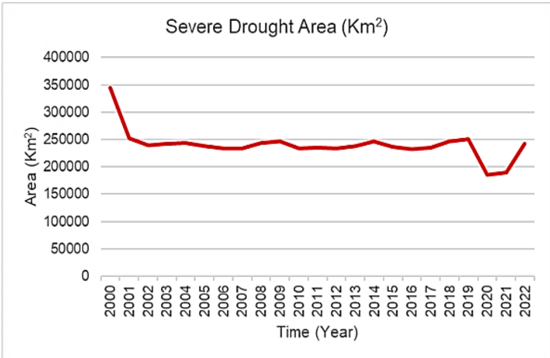

(c)

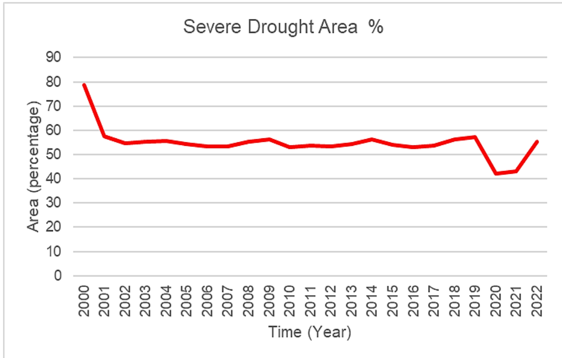

(d)

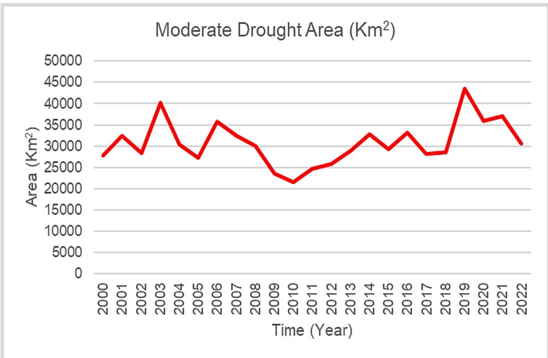

(e)

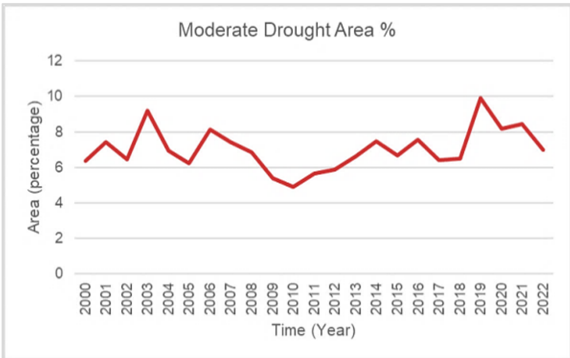

(f)

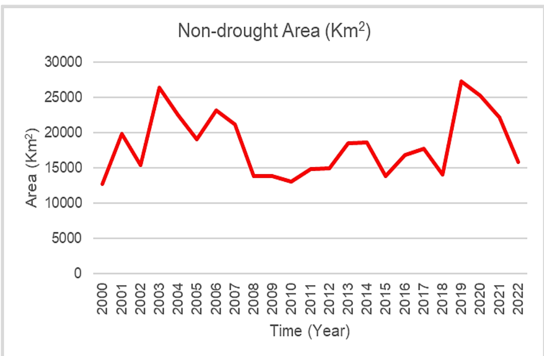

(g)

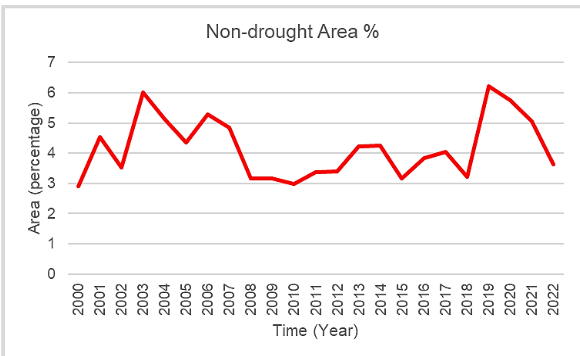

(h)

Figure 6: The time series of the LSWI for each class

The data from Figure 4 and Figure 6, as well as the following Figure 7, can be derived. That represents the relationships between the first side, extreme drought, and the second side, the temperatures and precipitations.

Figure 7a illustrates the relationship between the area of LSWI extreme drought class and the temperature, and there is increasing in the drought area concerning the increasing mean annual temperatures. The correlation coefficient between the extreme drought area and the temperatures was 0.98, representing a high correlation between the two factors. Figure 7b illustrates the relationship between the extreme drought area and the precipitations. The effect of precipitation can be seen as very high on the results of the extreme values. The correlation coefficient was 0.79, representing a high strength and direction of a relationship between the two variables.

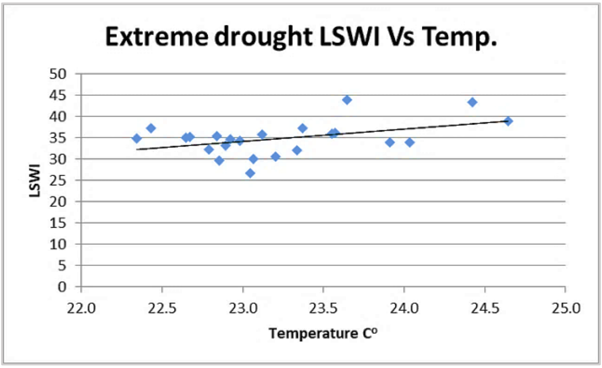

(a)

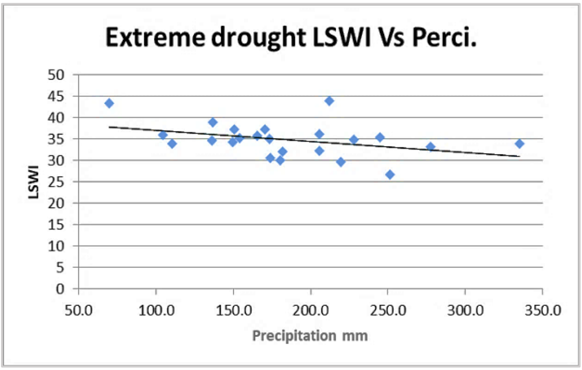

(b)

Figure 7: . The relationship between extreme drought and (a) temperatures and (b) precipitations

The findings of this research reveal an increasing trend in values over the years of study for extreme drought, moderate drought, and no drought, and there is a trend of decrease for severe drought. This trend leads to an increase in extreme droughts compared to other drought areas. The drought map from Figure 5 for 2019 is the least drought area compared with the different years because it has the greatest amount of precipitation this year, consistent with the results of Hassan and Al-Abadi [32]. On the other hand, the worst years were from 2020 to 2022 because they have the lowest annual precipitation and have increasing mean annual temperatures. This also coincided in the same period with the filling of the Turkish Ilisu Dam, which led to a decrease in water releases, which is consistent with the discussion of Al-Madhhachi et al. that the decline of water from the Tigris River will have impacts on the hydrological and environmental aspects [33]. Overall, it can be observed from the figures and tables that the hydrological drought will increase in the future, which requires the decision-makers to take steps against losing no drought areas and water bodies to extreme drought areas. The results show that the LSWI is an effective tool that uses satellite images to assess the hydrological drought. Although the LSWI and Landsat image data are available and can be used for hydrological drought assessment, they have many spatial and temporal resolution limitations. The spatial resolution of Landsat images (30 m) is considered a moderate resolution, so hydrological ground features with less than 30 meters, such as rivers and streams, cannot be detected accurately. The temporal resolution of the Landsat is approximately 16-18 days, which is considered a good resolution, but in case of any change in the wetland in this period will not be detected, and in case there is a high cloud cover in time, satellite visiting this will lead to neglect the captured image. The Landsat SWIR band can be used in different indices such as LSWI and NDVI. Although the LSWI is designed to detect the water in images and NDVI is used to detect the vegetation cover, the vegetation will have the same spectral fingerprint of water bodies spatially in the growing seasons. The LSWI is used mainly to map and classify water bodies. Still, if a flooded area can result from high rain (considered a temporary water body), the barren land will be registered as a water body, leading to false classification.

6. Conclusion

The impact of drought in Iraq was assessed in this study using remote sensing methods and the Land Surface Water Index (LSWI) over 23 years, from 2000 to 2022. Understanding how climate change will affect agriculture and water resources management is essential to fully grasp the research objective underlying Iraq's assessment of drought conditions through remote sensing and LSWI techniques. The manuscript provides valuable data on the spatial distribution and intensity of Iraq's 23-year drought that will help identify problem areas and develop mitigation measures. For this study, multi-temporal drought maps were created using Landsat satellite imagery with a spatial resolution of 30 meters. The study results show that the proportion of extreme drought is highest in the drought years 2020 and 2021 (43.9% and 43.3%, respectively). According to the analyzed images, the trend of extreme drought is increasing.

In contrast, the proportion of severe drought was highest in 2000 and 2001 (78.7% and 57.5%, respectively), and the trend of severe drought is decreasing. The most significant proportion of locations with moderate drought was observed in 2019 (9.9%) and 2003 (9.2%). Generally, the overall trend of the hydrological drought is increased, which is considered one of the most critical factors that lead to the deterioration of the agricultural economy, abandoning work in agriculture and livestock raising, and migration to the city to search for jobs with fixed salaries, which leads to the significant traffic congestion that exists in the capital, Baghdad. However, there are certain limitations to this study. The study relies on satellite imagery and LSWI data, which may have temporal and spatial resolution limitations. Future studies should consider merging new data sources and indicators, e.g., ground survey measurements such as soil water content data and socio-economic data such as economic losses and agricultural yields, to increase the accuracy and reliability of drought assessments. As a result, our work has shown that LSWI, in combination with remote sensing, is an efficient and cost-effective method for monitoring drought in Iraq.

Author contributions

Conceptualization, I. Mohammed. and I. Alawn.; data curation, I. Mohammed.; formal analysis, I. Alawn.; investigation, A. Ziboon.; methodology, I. Alawn.; project administration, I. Alawn., resources, I. Mohammed.; software, I. Mohammed.; supervision, I. Alawn. and A. Ziboon.; validation, I. Mohammed., I. Alawn. and A. Ziboon.; visualization, I. Mohammed.; writing—original draft preparation, I. Mohammed.; writing—review and editing, I. Alawn. All authors have read and agreed to the published version of the manuscript.

Funding

This research received no specific grant from any funding agency in the public, commercial, or not-for-profit sectors.

Data availability statement

The data that support the findings of this study are available on request from the corresponding author.

Conflicts of interest

The authors declare that there is no conflict of interest.

References

[1] N. Adamo, N. Al-Ansari, V. K. Sissakian, K. Fahmī, and S. A. Abed, Climate Change: droughts and increasing desertification in the Middle East, with special reference to Iraq, Engineering, 14 (2022) 235-273. https://doi.org/10.4236/eng.2022.147021

[2] A. H. Nama, I. A. Alwan, and Q. B. Pham, Climate change and future challenges to the sustainable management of the Iraqi marshlands, Environ. Monit. Assess., 196 (2024) 35. https://doi.org/10.1007/s10661-023-12168-8

[3] H. A. A. Gaznayee et al., Drought severity and frequency analysis aided by spectral and meteorological indices in the Kurdistan region of Iraq, Water, 14 (2022) 3024. https://doi.org/10.3390/w14193024

[4] L. W. Said, N. A. Aziz, and L. Y. Hussein, Spatiotemporal mapping of agricultural and meteorological drought in Wasit province based on GIS and remote sensing data, Ecol. Eng. Environ. Technol., 25 (2024) 115-122. http://dx.doi.org/10.12912/27197050/186869

[5] R. Niaz, F. Tanveer, M. Almazyad, I. Hussain, S. Alkhatib, and A. Y. Al-Razami, Characterization of meteorological drought using Monte Carlo feature selection and steady-state probabilities, Complexity, 2022 (2022) 1172805. https://doi.org/10.1155/2022/1172805

[6] V. Blauhut, M. Stoelzle, K. Stahl, and D. Hammerschmidt, Different drought types and the spatial variability in their hazard, impact, and propagation characteristics, Nat. Hazards Earth Syst. Sci., 22 (2022) 2099-2116. https://doi.org/10.5194/nhess-22-2099-2022

[7] Y. Pan, Y. Zhu, H. Lü, A.L. Yagci, X. Fu, E. Liu, H. Xu, Z. Ding, R. Liu, Accuracy of agricultural drought indices and analysis of agricultural drought characteristics in China between 2000 and 2019, Agric. Water Manag., 283 (2023) 108305. https://doi.org/10.1016/j.agwat.2023.108305

[8] Tallaksen, L. M. and H. A.J. van Lanen, Hydrological drought – processes and estimation methods for streamflow and groundwater, 2004.

[9] F. D. Kartika and P. Wijayanti, Drought disaster modeling using drought index: a systematic literature review, IOP Conf. Ser.: Earth Environ. Sci., 1190 (2022) 012026. http://dx.doi.org/10.1088/1755-1315/1190/1/012026

[10] L. Liuzzo, V. Puleo, S. Nizza, and G. Freni, Parameterization of a Bayesian Normalized Difference Water Index for Surface Water Detection, Geosciences, 10 (2020) 260. https://doi.org/10.3390/geosciences10070260

[11] Y. Xu et al., Drought in Shanxi Province Based on Remote Sensing Drought Index Analysis of Spatial and Temporal Variation Characteristics, Atmosphere, 14 (2023) 799. https://doi.org/10.3390/atmos14050799

[12] M. Behifar, A. A. Kakroodi, M. Kiavarz, and G. Azizi, Satellite-based drought monitoring using optimal indices for diverse climates and land types, Ecol. Inf., 76 (2023) 102143. http://dx.doi.org/10.1016/j.ecoinf.2023.102143

[13] G. Sofia, M. Sinatra, P. Tarolli, Enhancement of drought monitoring by means of soil sampling and drone-based multispectral sensing, EGU General Assembly Conference Abstracts, 2023, 24–28. https://doi.org/10.5194/egusphere-egu23-5230

[14] S. Cai, D. Zuo, H. Wang, Z. Xu, G. Wang, and H. Yang, Assessment of agricultural drought based on multi-source remote sensing data in a major grain-producing area of Northwest China, Agric, Water Manage., 278 (2023) 108142. https://doi.org/10.1016/j.agwat.2023.108142

[15] I. Hatem, I. A. Alwan, A. R. T. Ziboon, and A. Kuriqi, Assessment of agricultural drought in Iraq employing Landsat and MODIS imagery, Open Eng., 14 (2024) 20220583. http://dx.doi.org/10.1515/eng-2022-0583

[16] K. Chandrasekar, M. V. R. S. Sai, P. S. Roy, and R. S. Dwevedi, Land Surface Water Index (LSWI) response to rainfall and NDVI using the MODIS Vegetation Index product, Int. J. Remote Sens., 31 (2010) 3987-4005. https://doi.org/10.1080/01431160802575653

[17] K. Xiang, W. Yuan, L. Wang, and Y. Deng, An LSWI-Based Method for Mapping Irrigated Areas in China Using Moderate-Resolution Satellite Data, Remote Sens., 12 (2020) 4181. https://doi.org/10.3390/rs12244181

[18] Z. Dong, W. Zongming, L. Dianwei, R. Chunying, J. Mingming, and D. Zhi, Method for extracting wetland information based on a combination of NDVI and LSWI, 2014.

[19] Khalaf, A. G. Geospatial Modelling of Drought In Middle Euphrates Region Of Iraq Based On Remote Sensing And GIS Techniques. Ph.D. Civil Engineering, University of Technology-Iraq, 2019.

[20] I. A. Alwan, A. T. Ziboon, A. G. Khalaf, Q. B. Pham, D. T. Anh, and K. M. Khedher, Monitoring agricultural and meteorological drought using remote sensing, Arabian J. Geosci., 15 (2022) 1-15. http://dx.doi.org/10.1007/s12517-021-09407-y

[21] N. Al-Ansari, Topography and Climate of Iraq, J. Earth Sci. Geotech. Eng., 11 (2020) 1-13. https://doi.org/10.47260/jesge/1121

[22] Google. Landsat 7 Collection 1 Tier 1 8-Day TOA Reflectance Composite, Earth Engine Data Catalog. https://developers.google.com/earth-engine/datasets/catalog/LANDSAT_LE07_C01_T1_8DAY_TOA

[23] Google. USGS Landsat 8 Collection 2 Tier 1 TOA Reflectance, Earth Engine Data Catalog. https://developers.google.com/earth-engine/datasets/catalog/LANDSAT_LC08_C02_T1_TOA

[24] H. R. Safavi, V. Raghibi, O. Mazdiyasni, and M. Mortazavi-Naeini, A new hybrid drought-monitoring framework based on nonparametric standardized indicators, Hydrol. Res., 49 (2018) 222-26. https://doi.org/10.2166/nh.2017.266

[25] J. Bai, Y. Yu, and L. Di, Comparison between TVDI and CWSI for drought monitoring in the Guanzhong Plain, China, J. Integr. Agric., 16 (2017) 389-397. https://doi.org/10.1016/S2095-3119(15)61302-8

[26] Z. Hao and A. AghaKouchak, A Nonparametric Multivariate Multi-Index Drought Monitoring Framework, J. Hydrometeorol., 15 (2014) 89-101. https://doi.org/10.1175/JHM-D-12-0160.1

[27] X. Xiao et al., Satellite-based modeling of gross primary production in an evergreen needleleaf forest, Remote Sens. Environ., 89 (2004) 519-534. https://doi.org/10.1016/j.rse.2003.11.008

[28] X. Xiao et al., Satellite-based modeling of gross primary production in a seasonally moist tropical evergreen forest, Remote Sens. Environ., 94 (2005) 105-122. https://doi.org/10.1016/j.rse.2004.08.015

[29] R. Bajgain, X. Xiao, P. Wagle, J. Basara, and Y. Zhou, Sensitivity analysis of vegetation indices to drought over two tallgrass prairie sites, SPRS J. Photogramm. Remote Sens., 108 (2015) 151-160. https://doi.org/10.1016/j.isprsjprs.2015.07.004

[30] T. L. T. Du, D. D. Bui, M. D. Nguyen, and H. Lee, Satellite-based, multi-indices for evaluation of agricultural droughts in a highly dynamic tropical catchment, Central Vietnam, Water, 10 (2018) 659. https://doi.org/10.3390/w10050659

[31] I. A. Alwan and N. A. Aziz, Monitoring of surface ecological change using remote sensing technique over Al-Hawizeh Marsh, Southern Iraq, Remote Sens. Appl.: Soc. Environ., 27 (2022) 100784. https://doi.org/10.1016/j.rsase.2022.100784

[32] A. A. Hassan and A. M. Al-Abadi, Hydrological Assessment of Iraq for the Period 2002-2020 Using GRACE Terrestrial Water Storage Deficit, Iraq. Geol. J., 57 (2024) 120-142. https://doi.org/10.46717/igj.57.1A.11ms-2024-1-22

[33] A.-S. T. Al-Madhhachi, K. A. Rahi, and W. K. Leabi, Hydrological impact of ilisu dam on Mosul Dam; the river Tigris, Geosciences, 10 (2020) 120. https://doi.org/10.3390/geosciences10040120